System-Level Performance Gains of Selective Per-Antenna-Rate-Control (S-PARC)

Stephen J. Grant, Karl J. Molnar, and Leonid Krasny
Ericsson Research, P.O. Box 13969, 8001 Development Drive, RTP, NC 27709, USA
{stephen.grant, karl.molnar, leonid.krasny}@ericsson.com

Abstract— **Currently, there is a high level of interest in MIMO antenna systems, such as per-antenna-rate-control (PARC), for enhancing the data rates for the HSDPA provision of the WCDMA standard. Recent studies have shown that PARC may be improved by adaptively selecting the number of transmitted substreams (the MIMO mode) and the antenna subset from which the substreams are transmitted to better match propagation conditions. In this paper we evaluate the system-level performance of S-PARC for HSDPA. We show that S-PARC achieves significant gains with respect to conventional (non-selective) PARC as well as receive diversity systems, even in the presence of spatially correlated fading. We demonstrate the importance of MIMO mode and antenna selection in correlated fading, and show that without it, a performance loss with respect to receive diversity can occur.**

I. Introduction

Currently, there is a high level of interest in multiple-input-multiple-output (MIMO) antenna systems for enhancing the data rates for the high-speed-downlink-packet-access (HSDPA) provision of the WCDMA standard. Two such techniques that have attracted significant attention are (1) spatial-multiplexing, e.g., code-reuse (CR)-BLAST, a variant of the well known V-BLAST system [1], and (2) per-antenna-rate-control (PARC) [2], [3]. Both approaches transmit data substreams from all antennas simultaneously. However, recent studies have shown that performance can be improved by adapting both the number of transmitted substreams (i.e., the mode) and the subset of antennas from which the substreams are transmitted in order to better match propagation conditions. For example, [4] and [5] consider selection for spatial-multiplexing systems, and [6] considers a selective version of PARC (S-PARC).

While the gains due to selection have been established at the link-level, the literature contains little in the way of system-level evaluations of these schemes. In this paper, we assess the gains of S-PARC through system-level simulation in a practical HSDPA setting. This work builds upon our previous work reported in [7] in which we assess the system-level gains of CR-BLAST. Through system simulation, we are able to address the following important aspects not captured in a link evaluation:

- **SNR operating regime**. In general, the gains offered by MIMO are heavily dependent on SNR operating regime. Through simulation of a multicell system with multiple services, the operating regime is established since both own-cell and other-cell interference are modeled. The operating regime is further affected by the multiuser diversity obtained through user scheduling.
- **Antenna correlation**. It is well-known that the performance of MIMO schemes is sensitive to the correlation between antennas [8]. In this study we implement a version of the recently developed 3GPP spatial channel model [9] in our system simulator. Use of this model allows us to evaluate how well S-PARC adapts to the mobility of users as they experience differing correlation scenarios due to changing angle spreads and angles of departure, as well as differing delay spreads.
- **Hybrid ARQ (HARQ)**. Modeling retransmissions is crucial in order to properly establish user and system throughput.

II. Transmitter and Receiver Structures

Fig. 1 shows the S-PARC transmit structure used in this study. Here, the transmitter is configured for mode-N, i.e., $N \leq M$ data substreams are transmitted where M is the number of transmit antennas. The selected data rate for each substream is based on the feedback of channel quality indicators (CQIs) from the mobile. The CQIs are simply quantized versions of the SINRs at multiple stages of the successive interference cancellation receiver described below. Both the mode and the physical antennas on which the substreams are transmitted are adaptive, and the adaptation is based upon a maximization of the sum data rate across streams. In this way, the transmitter adapts to poor propagation conditions (e.g., low SNR, high antenna correlation) by selecting lower order modes, and good propagation conditions by selecting higher order modes.

In addition to the high-speed downlink shared channel (HS-DSCH) transmitted on N antennas, Fig. 1 also shows the transmission of a pilot on all M antennas to facilitate channel estimation at the receiver. A number of dedicated physical channels (DPCHs) are also transmitted from antenna 1 (for backwards compatibility). These include associated dedicated channels (ADPCHs) required for HS-DSCH operation, voice, control channels, etc. The multiple channelization codes used for the data substreams are reused on each active transmit antenna to avoid a code limitation problem; however, the pilot signals on all antennas are orthogonal.

In this study, the receiver is based on a combination of successive interference cancellation (SIC) and generalized-RAKE (GRAKE) concepts [10], and is specifically designed

0-7803-8887-9/05/$20.00 (c)2005 IEEE

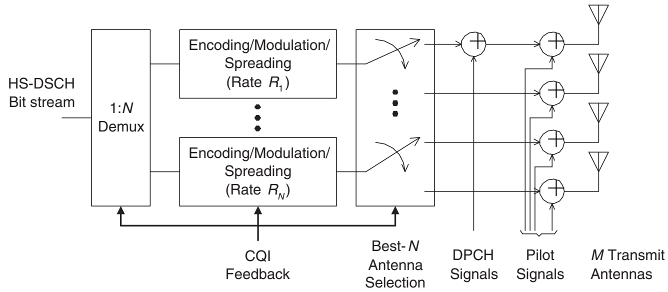

Fig. 1. S-PARC transmit structure for HSDPA showing the transmission of $N \leq M$ data substreams on the HS-DSCH.

to handle frequency-selective fading. The structure of the SIC-GRAKE receiver is fully described in [6]; however, we discuss the salient features here in order to understand the link adaptation process as well as the link-to-system interface.

The receiver front end is comprised of several banks of correlators (fingers), one for each of the K channelization codes used for the HS-DSCH. Each bank of fingers spans the multiple receive antennas, and the number of fingers per receive antenna is allowed to be greater than the number of channel tap delays. The extra fingers are used for the suppression of interference comprised of ISI/MAI from the data streams not yet cancelled through SIC as well as MAI from all non-HS-DSCH related channels, i.e., the DPCHs in Fig. 1. The interference is suppressed by treating it as colored Gaussian noise and exploiting its correlation across fingers in the design of the GRAKE combining weights. Since the interference level is different at each stage of SIC, the combining weights are necessarily different at each stage. We denote the combining weight vector for the nth stage as $\mathbf{w}_n$, where the length of this vector is equal to the total number of fingers spanning all receive antennas.

For link adaptation purposes, we desire an expression for the post-combining SINR for each stage of the SIC-GRAKE receiver. The number of stages in the receiver is strictly equal to the number of transmitted data streams N. Denote $c_{nk}(i)$ as the transmitted symbol on the kth channelization code of the nth data substream during the ith symbol period. The despread vector (correlator bank output) corresponding to this symbol is given by $\mathbf{y}_{nk}(i) = \mathbf{h}_n c_{nk}(i) + \mathbf{x}_{nk}(i)$ where $\mathbf{h}_n$ is the spatial net response vector. The net response vector is a function of the medium response between the physical antenna from which the nth data substream is transmitted and all receive antennas, as well as the chip-pulse autocorrelation function and finger delays (see [6, eq. (2)]).

The impairment vector $\mathbf{x}_{nk}(i)$ contains interference from all sources not related to the desired symbol $c_{nk}(i)$. This includes ISI/MAI from the K data codes used for substreams $\{n, n+1, \cdots, N\}$ (i.e., the ones not yet cancelled through SIC), MAI from the DPCHs transmitted from antenna 1, noise, and other-cell interference. We implement pilot subtraction in the receiver; hence, $\mathbf{x}_{nk}(i)$ does not include a pilot component. In this study we model the other-cell interference as spatially and temporally white.

The spatio-temporal covariance matrix of the impairment is denoted $\mathbf{R}_{\mathbf{x}}(n) = E\left[\mathbf{x}_{nk}(i)\,\mathbf{x}_{nk}^{\dagger}(i)\right]$ where $\dagger$ denotes Hermitian transpose. It is a function of the medium response between a subset of the transmit antennas and all receive antennas as well as the chip-pulse autocorrelation function and finger delays (see [6, eq. (3)]). It is also a function of the receiver input SNR $\gamma_o = E_c/I_o$ where E_c is the total received energy per-chip from all transmit antennas. This is a function of the total transmit energy as well as the path-loss and shadowing between the base station and a given user terminal. The quantity I_o is the power spectral density of the combined noise and other-cell interference (modeled as white).

The per-code post-combining SINR for the nth stage of SIC is determined by the ratio of the signal and noise components of the combiner output $\mathbf{z}_{nk}(i) = \mathbf{w}_n^{\dagger}\mathbf{y}_{nk}(i)$ and is given by

$$\rho_n = \frac{\mathbf{w}_n^{\dagger}\mathbf{h}_n E\left[|c_{nk}(i)|^2\right]}{\mathbf{w}_n^{\dagger} E\left[\mathbf{x}_{nk}(i)\,\mathbf{x}_{nk}^{\dagger}(i)\right]\mathbf{w}_n} = \mathbf{h}_n^{\dagger}\mathbf{R}_{\mathbf{x}}^{-1}(n)\,\mathbf{h}_n. \quad (1)$$

The latter equality follows from the former since the GRAKE combining weights are given by the vector $\mathbf{w}_n = \mathbf{R}_{\mathbf{x}}^{-1}(n)\,\mathbf{h}_n$.

III. System Simulation Approach

A. Link Adaptation

To enable link adaptation, the mobile terminals feed back quantized values of the per-stage SINRs $\{\rho_1, \rho_2, \cdots, \rho_N\}$ corresponding to the best transmit antenna selection for each possible mode $N \in \{1, 2, \cdots, M\}$. The best antenna selection for each mode is determined by considering all possible combinations of N antennas, and for each combination, the N SINRs are mapped to rates through a modulation and coding scheme (MCS) look-up table. The rates are then summed, and the antenna selection with the largest sum rate is selected. An indicator of this selection is fed back to the base station along with the corresponding SINRs. In this way, the mobile terminals perform antenna selection, but the base station is still able to select the mode.

The mode selection at the base station is also based on the maximum sum data rate; however other factors are typically taken into account. For example, the base has knowledge of available resources (power, codes) that may change from when the mobiles prepare their CQI reports. This could require rescaling of the reported SINRs thus requiring remapping of SINRs to rate in order to find the mode with the best sum rate. In addition the base station has knowledge of how much data is in queue for each user which may affect the selected mode, especially in bursty traffic conditions.

The MCS look-up table used for mapping per-stage SINRs to per-stream data rates contains a number of SNR-rate combinations plotted in Fig. 2. Each data rate corresponds to a particular combination of modulation type, number of channelization codes, and encoding rate for the WCDMA turbo code. In this study, the number of channelization codes K used for the HS-DSCH is fixed at 12. The modulation types used are QPSK and 16-QAM. The SNR switching point

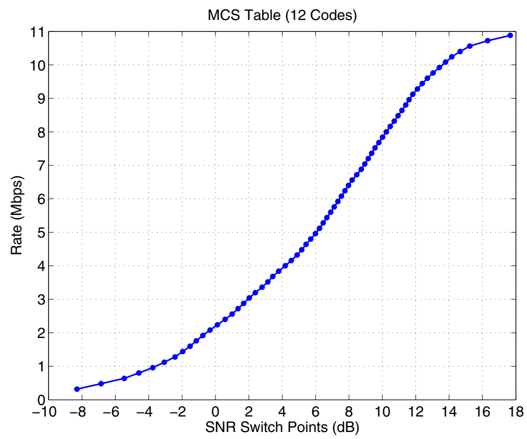

Fig. 2. MCS rates for 12 channelization codes with QPSK/16-QAM modulation.

for each MCS, i.e., the SNR below which a particular MCS is not allowed to be selected, is determined by simulating the block-error-rate (BLER) performance of the MCS in an AWGN channel. The switch point is defined as that SNR for which the BLER is equal to 10%.

B. Spatial Channel Model

In order to study the effects of antenna correlation, we consider two scenarios specified by the 3GPP spatial channel model (SCM) [9], namely the suburban macrocell and the urban microcell scenarios. The suburban macrocell scenario is broadly classified as narrow angle spread with variably light and heavy dispersion depending on the position of the mobiles in the cell. The urban microcell scenario, in contrast, is broadly classified as wide angle spread with light dispersion. In addition it contains a line-of-sight (LOS) component resulting in Rician fading.

In both cases, a modified version of the 3GPP SCM is implemented in order to overcome prohibitively large storage and computation requirements. The main parameters that affect spatial correlation, namely angle spread (AS), angle of departure (AoD), delay spread (DS), and Rician K-factor (K), are coarsely quantized to allow precomputation of a limited number of look-up tables containing the per-stage SINRs described previously. The SINRs in the look-up tables correspond to a large number of channel realizations that are generated using the SCM with the quantized values of AS, AoD, DS, and/or K. For each channel realization, the SINRs are precomputed for a range of input SNRs γ_o. Time variant angles of arrival (AoA) at the mobile terminals are accounted for by physically rotating the receive antenna orientation 360 degrees across the span of each look-up table.

During simulation, when the mobile positions are known, the AS, AoD, DS, and/or K parameters are generated according to the probability distributions specified by the 3GPP SCM and then quantized in order to index the appropriate look-up tables for each mobile. As the mobiles move, they index different positions in the tables. The appropriate SINRs at each index point are retrieved once the path-loss, shadowing, and other-cell interference power are known which together determine the input SNR γ_o. In this way, the variation of the spatial correlation across the cell is captured.

The important parameters for the suburban macrocell scenario are as follows. The delay spread (DS) is quantized to two values corresponding to the Pedestrian A power delay profile (light dispersion) or the Vehicular A profile (heavy dispersion). See [9] for the specification of these profiles. The angle spread (AS) at the base station is quantized to three values: 2, 5, and 8 degrees. The angle of departure (AoD) is quantized to two values: 12 and 48 degrees. The path loss model is $PL\,(dB) = 32.33 + 35.04\log_{10} d$ where d is the mobile to-base-distance. The cell radius is 1500 m.

The important parameters for the urban microcell scenario are as follows. A single delay spread (DS) value is used that matches the 3GPP SCM, resulting in light dispersion. However, the power-delay profile (PDP) used is an empirically designed 3-tap profile (plus LOS component) with fixed delays rather than the random delay model in [9]. The angle spread (AS) and angle-of-departure (AoD) are quantized to only one value: 19 degrees and 0 degrees, respectively. We chose such a coarse quantization since we found that the antenna correlation was insensitive to these parameters; the largest sensitivity was due to the Rician K-factor. Consequently, we quantize the K-factor to 6 values: -15, -10, -5, 0, 5, and 10 dB. During simulation, the K-factor is selected based on the mobile-to-base distance d. We found that the mean value of the K was between 0 and 5 dB. The path loss model for the non-line-of-sight (NLOS) component is $PL\,(dB) = 35.68 + 38.00\log_{10} d$ and for the LOS component is $PL\,(dB) = 30.62 + 26.00\log_{10} d$. Notice that the path loss exponent is significantly lower for the LOS component. One might imagine this to result in significant interference to other cells. However, the cell radius for the microcell environment is 500 m, and according to the SCM, the probability of a LOS component occurring decays linearly out to $d = 300$ m. Hence, a LOS component cannot occur for mobiles located greater than 300 m from the serving base which is less than the cell radius.

For both environments, the angle spread at the mobile is fixed at 70 degrees and the receive antenna spacing at 0.5λ. Three different transmit antenna spacings are considered, 10λ, 4λ and 0.5λ. However, we found little improvement in performance of the 10λ spacing compared to the 4λ spacing, hence performance results are presented only for the two closer spacings.

C. Simulation Parameters

Other important parameters for the HSDPA system simulation are as follows:

- 7 site layout with 1/3 sectorization (21 cells) with wrap-around to avoid edge effects; 500m cell radius; uniform user distribution; data users only (i.e., no voice users).
- Pilot power is 10% of maximum base station power for $M = 1$, 12.5% for $M = 2$, and 15% for $M = 4$

- Remainder of base station power (70-75%) allocated to HS-DSCH after power requirement is met for pilots, ADPCHs, and other overhead channels
- Hybrid ARQ employs Chase combining. Block error on any one stream forces retransmission of all streams.
- Continuous traffic model, i.e., full transmit buffers all of the time
- Proportional fair scheduling
- User mobility 3 km/h
- Error-free CQI feedback; non-ideal link adaptation modeled through 2 TTI feedback delay (4 ms)

D. Performance Measures

The two performance measures we consider are user and system throughput, obtained as the offered load is varied as 1, 2, 5, 10 users/cell. User throughput is defined as the number of correctly delivered bits (accounting for retransmissions) divided by the simulation time. User throughput is a random variable across the ensemble of users, and we choose the 90th percentile measure which serves as a lower bound on the performance for the 10% best users. System throughput is the number of correctly delivered bits to all users in the system normalized by the total number of cells.

For reference we generate throughput results for a single-input-single-output (SISO) system as well as a receive diversity (RxDiv) system with the same number of receive antennas as S-PARC. The latter is an important reference to establish whether the investment of extra transmit antennas is worthwhile. The receiver used for both SISO and RxDiv is a special case of the SIC-GRAKE receiver used for S-PARC in that only one stage is required. In addition, we compare the performance of S-PARC to conventional (non-selective) PARC where mode-M is transmitted exclusively.

IV. Results and Conclusions

Figs. 3–8 show the performance of S-PARC for the 4×4 and 4×2 antenna configurations. Clearly, S-PARC offers significant gains with respect to both SISO and RxDiv. Comparing the two environments, the urban microcell environment offers better absolute throughputs due to the low delay spread and the large angle spread which results in low antenna correlation. Relatively speaking, the 4×4 S-PARC system with 4λ antenna spacing achieves a 3.5 (2.8) factor improvement in the macrocell (microcell) environment compared to SISO at a load of 2 users/cell (2nd point on each curve). For the 4×2 S-PARC system, the improvement factor is 1.8 for both environments.

Even when the antenna spacing is reduced from 4λ to 0.5λ, thus increasing the antenna correlation, S-PARC still achieves a gain with respect to RxDiv. Moreover, in the microcell scenario, there is very little degradation with tight spacings due to the low antenna correlation in wide angle spread. Interestingly, even with a LOS component, the presence of the diffuse component offers enough effective subchannels over which to transmit multiple streams and thus achieve a rate gain.

These results illustrate the importance of mode selection for S-PARC used to adapt to different antenna configurations, SNRs, and correlation scenarios. From Fig. 5, one can see that as the antenna spacing decreases (correlation increases) modes 3 and 4 are selected much less frequently in favor of the lower-order modes in the suburban macrocell environment. For the 4×2 configuration in the macrocell environment (Fig. 8) one can see that modes 1 and 2 are used almost exclusively, since the receiver has only two antennas. However, when the antenna spacing is reduced, mode 1 is selected more frequently than mode 2. In the microcell environment, on the other hand, the antenna spacing has very little impact on the mode selection due to the low correlation values. All of this is consistent with theory that says that as correlation increases, the effective number of subchannels through which to signal is reduced. S-PARC adapts to this automatically by transmitting fewer streams [8].

In contrast to the above conclusions, conventional (non-selective) PARC runs into problems when the number of receive antennas is less than the number of transmit antennas and/or the antenna correlation is quite large. For example, in Fig. 6, one can see that PARC offers only marginal gains with respect to RxDiv. Moreover, for very close antenna spacings PARC actually suffers a degradation. We note that the use of PARC in balanced antenna configurations (e.g., 4×4) can achieve a large fraction of the gains of S-PARC, especially in the lightly dispersive, wide angle spread scenarios (i.e., urban microcell).

References

[1] G. Foschini, G. Golden, R. Valenzuela, and P. Wolniansky, "Simplified processing for high spectral efficiency wireless communication employing multi-element arrays," *IEEE J. Select. Areas Commun.*, vol. 17, pp. 1841–1852, Nov. 1999.

[2] M. K. Varanasi and T. Guess, "Optimum decision feedback multiuser equalization with successive decoding achieves the total capacity of the Gaussian multiple-access channel," in *Proc. Assilomar Conf. on Signals, Systems, and Computers*, Monteray, CA, Nov. 1997, pp. 1405–1409.

[3] S. T. Chung, A. Lozano, and H. C. Huang, "Approaching eigenmode BLAST channel capacity using V-BLAST with rate and power feedback," in *Proc. IEEE VTC'01-Fall*, Atlantic City, NJ, Oct. 2001.

[4] R. W. Heath Jr. and D. J. Love, "Multi-mode antenna selection for spatial multiplexing systems with linear receivers," in *Proc. of Allerton Conf. on Commun., Cont., and Comp.*, Monticello, IL, Oct. 2003.

[5] R. Narasimhan, "Spatial multiplexing with transmit antenna and constellation selection for correlated MIMO fading channels," *IEEE Trans. Sig. Proc.*, vol. 51, p. 2829, Nov. 2003.

[6] S. Grant, J.-F. T. Cheng, L. Kransny, K. Molnar, and Y.-P. E. Wang, "Per-Antenna-Rate-Control (PARC) in frequency selective fading with SIC-GRAKE receiver," in *Proc. IEEE VTC'04-Fall*, Los Angeles, CA, Sept. 2004.

[7] K. J. Molnar, S. J. Grant, L. Kransy, and E. Englund, "Improved packet data performance for WCDMA using multi-antenna techniques," in *Proc. IEEE VTC'03-Fall*, Orlando, FL, Oct. 2003.

[8] D.-S. Shiu, G. J. Foschini, M. J. Gans, and J. M. Kahn, "Fading correlation and its effect on the capacity of multielement antenna systems," *IEEE Trans. Commun.*, vol. 48, pp. 502–513, Mar. 2000.

[9] 3rd Generation Partnership Project, "TSG RAN WG1, Spatial Channel Model for Multiple Input Multiple Output (MIMO) Simulations, TR 25.996 v.6.1.0," Sept. 2003.

[10] G. E. Bottomley, T. Ottosson, and Y.-P. E. Wang, "A generalized RAKE receiver for interference suppression," *IEEE J. Select. Areas Commun.*, vol. 18, pp. 1536–1545, Aug. 2000.

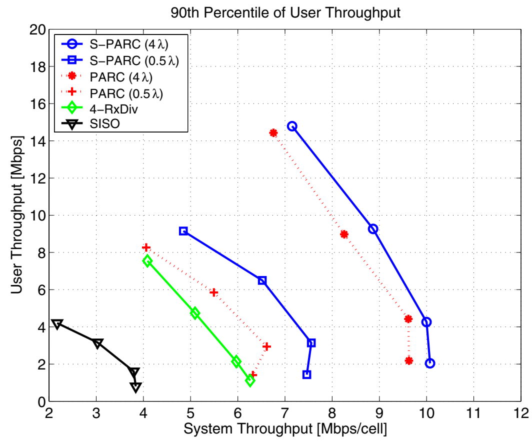

Fig. 3. Throughput for 4×4 system in suburban macrocell environment.

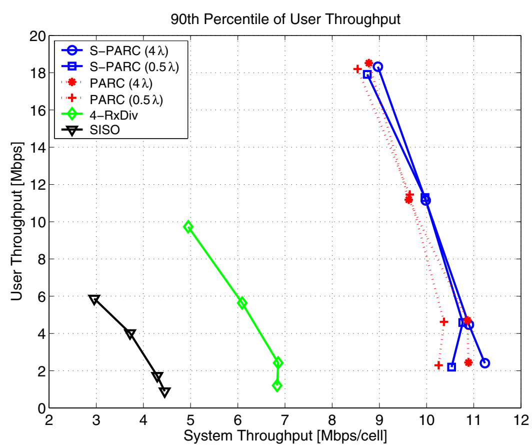

Fig. 4. Throughput for 4×4 system in urban microcell environment.

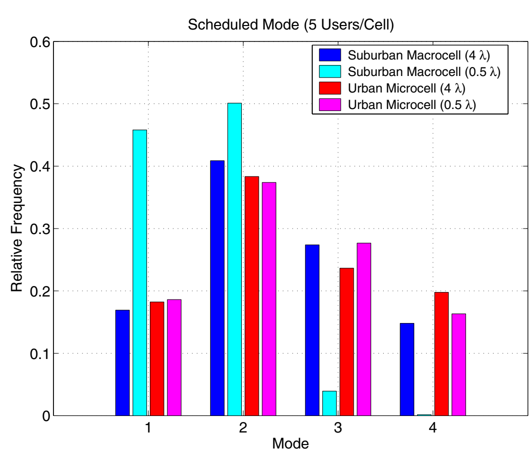

Fig. 5. Histogram of the selected mode for 4×4 S-PARC system in suburban macrocell and urban microcell environments.

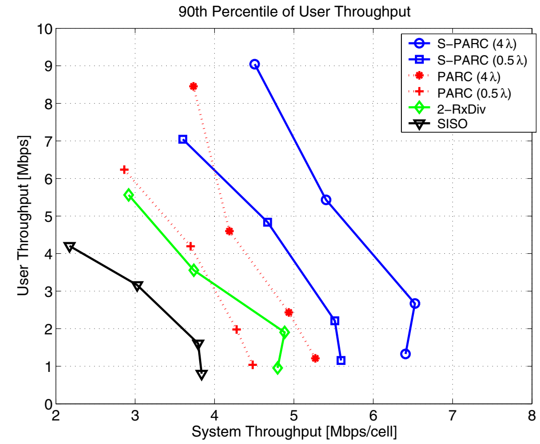

Fig. 6. Throughput for 4×2 system in suburban macrocell environment.

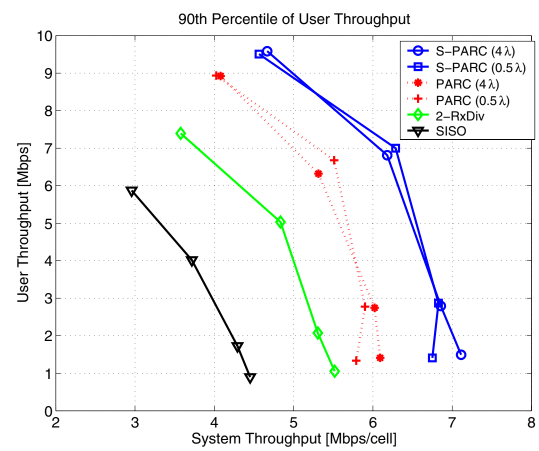

Fig. 7. Throughput for 4×2 system in urban microcell environment.

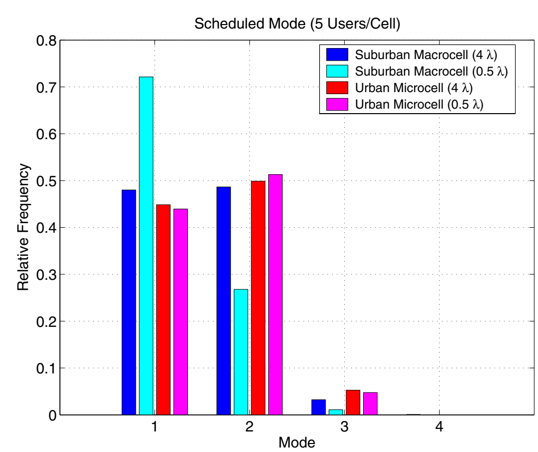

Fig. 8. Histogram of the selected mode for 4×2 S-PARC system in suburban macrocell and urban microcell environments.